Research Article

Nickel-Silicon Related Color Center Formed in Nanodiamond Grains under CVD Growth

Sára Tóth, László Himics, and Margit Koós

Institute for Solid State Physics and Optics, Wigner Research Center for Physics, Hungarian Academy of Sciences, P.O. Box 49, Budapest 1525, Hungary

Correspondence should be addressed to Sára Tóth; toth.sara@wigner.mta.hu

Formation of optical centers in nanodiamond grains with narrow, near-infrared emission at room temperature is one of the most important challenges nowadays. Our aim was to form a metal-related color center through the CVD growth process of nanodiamond. Previously undocumented photoluminescence (PL) system with 865 nm zero-phonon line (ZPL) and 2 nm full width at half maximum (FWHM) was successfully created in nanodiamond grains. According to the detailed analysis of the spectral features of the ZPL and quasilocal modes of the vibronic sideband, a complex center containing Ni and Si atoms could be accounted for these PL features. The inclusion of Ni and Si impurity atoms in the complex optical center was strengthened by micro-Raman spectroscopy performed in the frequency range due to quasilocal vibrations of the vibronic sideband.

1. Introduction

In the last decades, production of highly luminescent color centers in nanometer sized diamond is one of the most interesting research fields due to the unique properties of nanocrystalline diamond, like biocompatibility, chemical stability, and inertness. Some high quality applications, such as quantum technology [1–3] or biological imaging [4], are in the focus nowadays; however, development of reliable single-photon source working at room temperature is still the main challenge for research groups. It is well known that emission of color centers related to different impurities within the diamond crystal lattice covers the spectral range from deep ultraviolet to far infrared. Metal-related impurity centers are particularly interesting due to their relatively low electron-phonon coupling resulting in a narrow (generally 5–15 meV) and highly intensive ZPL and a weak vibronic sideband. The estimated Huang-Rhys factor of these centers was found to be as low as $S \leq 1$.

During the last years, nickel-related centers gained much attention as one-photon emitters with high saturation counting rate in the near infrared region. In low nitrogen content diamond, the most common nickel-related center has PL doublet around 883/885 nm [5, 6], which is in connection with ground state splitting caused by the spin orbital interaction. Nickel-nitrogen complex (NEx) centers were observed in high nitrogen content diamond and the structure of some centers has been determined using EPR technique [7, 8]. The paramagnetic NE8 optical center (one nickel atom surrounded by four equivalent nitrogen atoms in the coordination shell) is responsible for the 793.6 nm vibronic system in absorption and luminescence [7, 9, 10]. Nickel-silicon complexes with emission at around 770 nm were identified in samples created by focused ion beam implantation of nickel [11] and ion implantation of nickel and silicon to type IIa CVD diamond [12]. CVD growth of diamond films has demonstrated production of a wide range of nickel-, silicon-, and nitrogen-related defects as one-photon emitters [13, 14].

Metallic impurity centers in diamond could be created in different ways. The ion implantation technique is a widely used method for a large number of applications. This process offers high diversity in the palette of incorporated atoms, but it arrived to its limits according to the spatial resolution and the positioning. Moreover, nanocrystalline samples could not be implanted effectively because the accelerated ions always cause damage in the crystal lattice (radiation defects), which could be restored partially only with high temperature annealing [15]. Another way to create impurity centers in

the diamond lattice is the CVD growth process, which has some unique advantages, like simplicity, flexibility, and control over the incorporation of impurities. Metallic centers, like NE8 [10, 16], Cr [17], and W [18], were successfully created by CVD method in the last years.

Fluorescent nanodiamond possesses unique properties with respect to their application in quantum communication, quantum photonics, and biological imaging as well as in the implementation of several methods in nanoscopy. These properties generate a demand on the creation of color centers of favorable properties in nanodiamond. In this paper, we report on the formation of infrared emitting defect center in nanodiamond grains of 120 nm average size. This previously undocumented PL system emits a narrow-bandwidth, highly intensive ZPL at 865 nm (1.433 eV) with 2 nm (3 meV) FWHM at room temperature. Identification and assignation of this near infrared emitter to a given defect structure could be performed by the analysis of emission properties. Color center could be unambiguously characterized by the ZPL and the vibronic sideband together, even if the ZPL of different impurities are very close to each other [19]. Our results of high intensity and narrowness of the ZPL measured in several diamond nanograins suggest that this color center could be related to metal impurity. In the wavelength region (800–900 nm) of the ZPL peak position (865 nm), several spectral lines have been observed [14] in CVD diamond films and the zero-phonon lines have been correlated with previously identified Ni and Ni-Si complex related centers. The vibronic sideband characterizing the electron-vibration coupling at optical center is dominated by energies < 70 meV in the case of 865 nm PL system. These vibration energies below the low frequency acoustic modes of diamond indicate the coupling electronic transition to quasilocal vibration modes. To get more insight into these quasilocal vibrations and especially to determine impurity atoms taking part in these quasilocal vibrations, micro-Raman spectroscopy in low frequency range ($<500 \, cm^{-1}$) was used.

2. Materials and Methods

2.1. Sample Preparation. Nanodiamond grains with the average size of 120 nm were grown from a mixture of CH_4 and H_2 using microwave (2.45 GHz) chemical vapor deposition process. Si wafers served as substrates through the bias-enhanced nucleation and growth process. The chamber pressure was kept at 40 mbar and the microwave power was 1200 W. The total gas flow and the methane ratio were 100 sccm and 0.2%, respectively, while the substrate temperature was 700°C. The source of the Ni is the reaction chamber itself made from austenitic stainless steel (DIN 1.4541), which contains usually 9–12% nickel, while the source of the Si was crystalline silicon, which serves as a substrate.

2.2. Sample Characterization. The morphology of the nanograins was investigated by using a LEO 1540 XB field emission scanning electron microscope. Renishaw 1000 B micro-Raman spectrometer attached to a Leica DM/LM microscope was used to examine emitted light and Raman scattering at room temperature. The 488 nm line of an Ar-ion laser

FIGURE 1: Scanning electron micrograph of nanodiamond grains.

served as an excitation source for PL measurements. Spectral distribution of the emitted light was analyzed in the 800–900 nm emission wavelength region with spectral resolution of $1 \, cm^{-1}$. Raman scattering measurements were performed in the wavenumber range of 50–500 cm^{-1} with 785 nm diode laser excitation. Color center of 865 nm ZPL was found by the scanning of nanodiamond grains. The emitted light and Raman scattering spectrum were measured in the same position. The diameter of the illuminated spot was 1 μm.

3. Results and Discussion

Numerous nanodiamond grains were scanned and approximately every third grain possesses the 865 nm PL system, which proved to be stable at room temperature. The distribution of nanodiamond grains on the silicon substrate material is inhomogeneous as it is clearly seen in the scanning electron micrograph (Figure 1).

Fine structure of the ZPL with 0.2–0.3 meV energy spacing between each line was also measured (see Figure 2 inset) in some nanodiamond grains indicating the presence of single center in these grains. Figure 2 shows the emission of 865 nm PL system measured on nanodiamond grains at room temperature. The highly intensive narrow-bandwidth luminescence at 865 nm with 2 nm (3 meV) FWHM possesses a vibronic sideband of very low intensity. Both of the narrow-bandwidth ZPL and the vibronic sideband feature correspond to a weak electron-vibration coupling at the optical center. Some scattering of the ZPL position (~1 nm) has been observed in different nanodiamond grains, although the majority of the measured color centers emit at 865 nm ZPL position. Even at room temperature, the emitted light is concentrated in the ZPL, and by using Lorentzian fitting of the ZPL the estimated Huang-Rhys factor (S) in the 860–900 nm wavelength region was found to be as low as 0.097. This small value indicates the presence of heavy impurities in this color center, because generally they tend to exhibit low electron-vibration coupling [19]. The observed spectral features—narrow bandwidth, fine structure of the ZPL, and small H-R factor—indicate the metal impurity content of the optical center. According to the literature data [11–14], Ni-based color centers have intensive emission in this wavelength region, but those are differing from the 865 nm
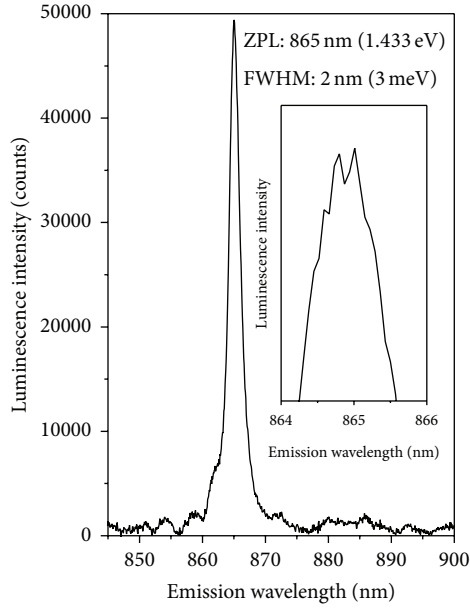
FIGURE 2: Spectral feature of the 865 nm PL system excited by 488 nm at room temperature in nanodiamond grains prepared through the CVD growth process. The inset shows the fine structure of the 865 nm ZPL.
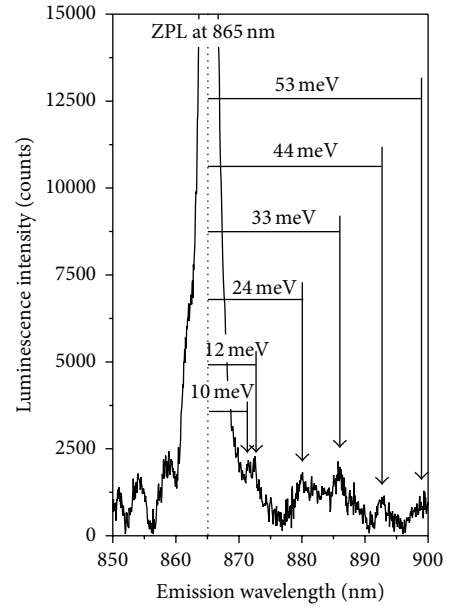

FIGURE 3: Vibronic sideband structure of the 865 nm ZPL shown on a stretched intensity scale compared to Figure 2. The observed sideband features are marked and those energies are signed in meV with respect to the ZPL peak position.

PL system. Identification of the structure and the impurity content of the color center require a detailed analysis of the vibronic sideband.

Spectral feature of the 865 nm PL system can be seen on Figure 3 in a stretched intensity scale compared to Figure 2 in order to show more clearly the weak vibronic sideband structure. Dominant vibrational mode coupled to the electron transition could not be observed, as the intensity of every ZPL replica is very similar and their distinct energetic spacing from ZPL peak position is clearly seen in Figure 3. The energies of the vibrations coupled to electron transition are low and they cover the range from 10 meV up to 53 meV. According to the behavior of the phonon density of states in diamond, namely, the cut-off at around 165 meV and strongly decreasing below 70 meV [19, 26, 27], all sideband features above 165 meV and below 70 meV are related to local and quasilocal modes, respectively. Analysis of the vibronic sideband structure in this energy region could give information about local and quasilocal vibrations and therefore about those impurities which are involved in the emission itself.

The vibrational modes coupled to electron transition at optical center, which accounts for the 865 nm PL system (see Figure 3), are differing from the diamond lattice modes and those can be considered as quasilocal vibrations characterizing the optical center. The small values of vibration energies indicate the incorporation of a heavy impurity atom into the optical center. Since the emission in the wavelength region between 800 and 900 nm is mostly related to optical centers containing Ni impurity atom, it seems to be obvious to calculate possible energies of quasilocal vibrations related to some defect center containing Ni impurity atom. Under CVD deposition process, the Ni impurity atoms through

the plasma etching of stainless steel chamber could be incorporated into nanodiamond grains. Regarding the incorporation of silicon impurity from the substrate material into diamond grains through the growth process, silicon impurity atom as defect center component could also be taken into account. If a defect center contains heavy impurity atom of a mass, M_I considerably exceeding the mass of the host atom M_C can generate only quasilocal vibrations involving this impurity [19]. Supposing that the impurity atom does not noticeably change the forces of interatomic interactions inside the defect, the frequency (ω_{QL}) and resonance width ($\Delta\omega_{QL}$) of the quasilocal vibration could be estimated by the following expressions:

$$\omega_{QL} = \omega_D \sqrt{\frac{M_C}{3\left(nM_I - M_C\right)}},$$

$$\Delta\omega_{QL} = \frac{\pi}{6}\omega_D \frac{M_C}{nM_I - M_C}, \tag{1}$$

where $\omega_D = 150$ meV is the Debye frequency of the diamond lattice, M_I and M_C are the masses of the impurity and carbon atoms, respectively, and n is the number of impurity atoms involved in the quasilocal vibration [28]. In Table 1, the calculated frequency and resonance width of quasilocal vibrations for some possible defects containing heavy impurity atom are summarized.

To gain more insight into the atomic model of defect center, it is worthwhile to compare experimental results with calculated vibration energies given in Table 1. Vibronic sideband of 865 nm ZPL exhibits features with a separation of 24, 33, and 44 meV energies. The weak peak separated by 53 meV energy from the 865 nm ZPL corresponds also

TABLE 1: Calculated vibration energy and resonance width of quasi-local vibrations for some possible defects containing heavy impurity atom.

| ω_{QL} (meV)	$\Delta\omega_{QL}$ (meV)	Impurity content
43.9	20.2	1Ni
29.2	8.9	2Ni
23.4	5.7	3Ni
34.7	12.6	1Ni + 1Si
26	7.1	2Ni + 1Si
23.6	5.8	2Ni + 2Si
29.6	9.2	1Ni + 2Si

FIGURE 4: Raman spectrum of nanodiamond grain in the low frequency region excited by 785 nm diode laser. The spectrum was measured on the same spot of focused laser beam, from where the 865 nm PL system was detected. The peak positions are given in cm^{-1}. The assignments of the peaks and their references are given in Table 2.

to an interaction with quasilocal vibration at optical center. The calculated value of 29.2 meV for the defect center of 2Ni impurity content (Table 1) lies between the two peaks of 24 and 33 meV which was experimentally observed. It is interesting that the 2.56 eV nickel-related center exhibits narrow bands separated from the ZPL by energies of 24 and 36 meV similarly to our results, which was assigned to two types of quasilocal vibration involving two nickel atoms [19]. The atomic structure of the optical center accounting for the 865 nm (1.433 eV) PL system should be different from the previously described structure because of the ZPL peak position as well as the difference in the details of the vibronic sideband structure. The calculated value of the quasilocalized vibration energy is 34.7 meV and 23.6 meV for atomic models involving 1Ni + 1Si and 2Ni + 2Si impurity atoms, respectively (Table 2). At the same time, the calculated vibration energy of 43.9 meV for defect involving one Ni atom approaches the peak energy of 44 meV in the vibronic sideband. This tentative description provides only some atomic structure; however, the atomic model of optical center as a whole exhibits all the experimentally measured peaks in the vibronic sideband. Therefore, it is worthwhile to monitor quasilocal vibrations by using an effective and nondestructive method, the Raman scattering measurements. This study detects only the Raman active modes among the quasilocal vibrations.

Figure 4 shows Raman scattering spectrum in low frequency region (50–500 cm^{-1}) measured on the same spot of focused laser beam, from where the 865 nm PL system was detected. The several scattering bands in the Raman spectrum characterize the bonding structure in the excited volume of nanocrystalline grains including the optical center. The peak positions of Raman spectrum, their structural assignment, and references are given in Table 2. Experimental results for peak positions in vibronic sideband of 865 nm ZPL are also indicated in meV in the last column of Table 2. The atomic structure of the species, to which Raman peaks are assigned, contains Ni or Ni and Si atoms, which are considered as heavy impurity in diamond lattice. These impurity atoms contribute to quasilocal vibrations at optical centers. The NiC$_3$ asymmetric (9.7 meV) and symmetric (14.4 meV) deformation modes energies [20] are close to the sideband peaks of 10 and 12 meV of 865 nm ZPL. Quasilocalized vibration of 141 cm^{-1} (17.5 meV) assigned to Ni$_2$Si atomic structure [21–24] does not contribute to vibronic sideband of the studied ZPL system. Vibrations in the 181–407 cm^{-1} range
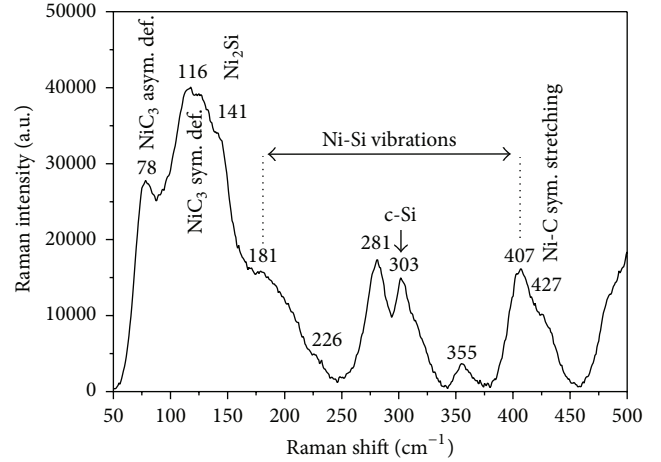
are assigned to NiSi species [21–24], while the Raman peak of 427 cm^{-1} is related to Ni-C symmetric stretching mode [20]. Raman peak at 303 cm^{-1} is assigned to crystalline silicon wafer under the stress caused by the nanodiamond film [25]. Among the observed Raman active quasilocal vibrations, four of them, the bands of 181 cm^{-1} (22.4 meV), 281 cm^{-1} (34.8 meV), 355 cm^{-1} (44 meV), and 407 cm^{-1} (50.5 meV), are also observed in the vibronic sideband of 865 nm ZPL (see Table 2). On the basis of this argumentation, the bonding model of optical center accounts for the 865 nm PL system containing Ni and Si impurity atoms together.

Additional measurements are needed to identify definitely the structure of the color center, since Ni ions could occupy substitutional [29], interstitial [30], and divacancy [31] position equally. One possible approach could be as follows: Ni occupies one of the two vacancy positions in the SiV color center and the local strain caused by large Ni atom relaxes by movement of silicon atom into the direction of the other vacancy position. This tentative picture could be supported by the experimental observation that the emission intensity of SiV center is very strong in grains where the 865 nm ZPL is completely absent, while in the other grains both of the two centers possess similar emission intensity.

4. Conclusion

Infrared light emitting color center was formed in nanodiamond grains through CVD deposition process. Previously undocumented PL system emits highly intensive narrow-bandwidth ZPL at 865 nm (1.433 eV) of 2 nm (3 meV) FWHM. Fine structure of ZPL with 0.2 and 0.3 meV separation between component lines was measured in grains containing only one optical center. The estimated Huang-Rhys factor of 0.097 indicates heavy impurity atom included in the optical center. The vibronic sideband of 865 nm ZPL

TABLE 2: The peak positions of Raman scattering spectrum, their assignment to atomic bonding species, and references are summarized. In the last column, the peak positions of the vibronic sideband of the 865 nm ZPL are given.

Raman peaks (cm^{-1})	Raman peaks (meV)	Assignments and references	Peaks of PL vibronic sidebands (meV)
78	9.7	NiC$_3$ asym. deformation [20]	10
116	14.4	NiC$_3$ sym. deformation [20]	12
141	17.5	Ni$_2$Si [21–24]	
181	22.4		24
226	28	NiSi [21–24]	
281	34.8		33
303	37.6	c-Si [25]	
355	44	NiSi [21–24]	44
407	50.5		53
427	52.9	Ni-C sym. stretching [20]	53

is dominated by quasilocalized vibrations due to heavy impurity atoms that constitute the optical center. The calculation of quasilocal vibration frequencies of vibronic sideband provides information about the heavy impurity atom content of the optical center. Raman scattering study performed in low frequency region confirmed that the optical center contains Ni and Si atoms together.

Conflict of Interests

The authors declare that there is no conflict of interests regarding the publication of this paper.

Acknowledgment

References

[1] C. Kurtsiefer, S. Mayer, P. Zarda, and H. Weinfurter, "Stable solid-state source of single photons," *Physical Review Letters*, vol. 85, no. 2, article 290, 2000.

[2] A. Beveratos, R. Brouri, T. Gacoin, A. Villing, J.-P. Poizat, and P. Grangier, "Single photon quantum cryptography," *Physical Review Letters*, vol. 89, no. 18, Article ID 187901, 2002.

[3] F. Jelezko, T. Gaebel, I. Popa, M. Domhan, A. Gruber, and J. Wrachtrup, "Observation of coherent oscillation of a single nuclear spin and realization of a two-qubit conditional quantum gate," *Physical Review Letters*, vol. 93, no. 13, Article ID 130501, 2004.

[4] D. Ho, Ed., *Nanodiamonds: Applications in Biology and Nanoscale Medicine*, Springer, 2010.

[5] M. H. Nazaré, A. J. Neves, and G. Davies, "Optical studies of the 1.40-eV Ni center in diamond," *Physical Review B*, vol. 43, no. 17, pp. 14196–14205, 1991.

[6] K. Iakoubovskii and G. Davies, "Vibronic effects in the 1.4⁻ eV optical center in diamond," *Physical Review B*, vol. 70, no. 24, Article ID 245206, 8 pages, 2004.

[7] V. A. Nadolinny, A. P. Yelisseyev, J. M. Baker et al., "A study of ^{13}C hyperfine structure in the EPR of nickel-nitrogen-containing centres in diamond and correlation with their optical properties," *Journal of Physics: Condensed Matter*, vol. 11, no. 38, pp. 7357–7376, 1999.

[8] A. T. Collins, H. Kanda, J. Isoya, C. A. J. Ammerlaan, and J. A. van Wyk, "Correlation between optical absorption and EPR in high-pressure diamond grown from a nickel solvent catalyst," *Diamond and Related Materials*, vol. 7, no. 2–5, pp. 333–338, 1998.

[9] T. Gaebel, I. Popa, A. Gruber, M. Domhan, F. Jelezko, and J. Wrachtrup, "Stable single-photon source in the near infrared," *New Journal of Physics*, vol. 6, article 98, 2004.

[10] J. R. Rabeau, Y. L. Chin, S. Prawer, F. Jelezko, T. Gaebel, and J. Wrachtrup, "Fabrication of single nickel-nitrogen defects in diamond by chemical vapor deposition," *Applied Physics Letters*, vol. 86, no. 13, Article ID 131926, pp. 1–3, 2005.

[11] I. Aharonovich, C. Zhou, A. Stacey et al., "Enhanced single-photon emission in the near infrared from a diamond color center," *Physical Review B*, vol. 79, Article ID 235316, 2009.

[12] D. Steinmetz, E. Neu, C. Hepp et al., "Single-photon emission from Ni-related color centers in CVD diamond," in *Quantum Optics, 77270P*, vol. 7727 of *Proceedings of SPIE*, June 2010.

[13] S. Castelletto, A. Edmonds, T. Gaebel, and J. Rabeau, "Production of multiple diamond-based single-photon sources," *IEEE Journal on Selected Topics in Quantum Electronics*, vol. 18, no. 6, pp. 1792–1798, 2012.

[14] S. Castelletto and A. Edmonds, "680–890 nm spectral range of nickel-nitrogen and nickel-silicon complex single centres in diamond," in *Quantum Communications and Quantum Imaging X*, vol. 8518 of *Proceedings of SPIE*, October 2012.

[15] C. Uzan-Saguy, C. Cytermann, R. Brener, V. Richter, M. Shaanan, and R. Kalish, "Damage threshold for ion-beam induced graphitization of diamond," *Applied Physics Letters*, vol. 67, article 1194, 1995.

[16] M. Wolfer, A. Kriele, O. A. Williams, H. Obloh, C.-C. Leancu, and C. E. Nebel, "Nickel doping of nitrogen enriched CVD-diamond for the production of single photon emitters," *Physica Status Solidi (A)*, vol. 206, no. 9, pp. 2012–2015, 2009.

[17] I. Aharonovich, S. Castelletto, D. A. Simpson et al., "Two-level ultrabright single photon emission from diamond nanocrystals," *Nano Letters*, vol. 9, no. 9, pp. 3191–3195, 2009.

[18] S. Lal, T. Dallas, S. Yi, S. Gangopadhyay, M. Holtz, and F. G. Anderson, "Defect photoluminescence in polycrystalline diamond films grown by arc-jet chemical-vapor deposition," *Physical Review B*, vol. 54, no. 19, pp. 13428–13431, 1996.

[19] A. M. Zaitsev, "Vibronic spectra of impurity-related optical centers in diamond," *Physical Review B*, vol. 61, no. 19, pp. 12909–12922, 2000.

[20] G. M. Howell and J. Edwards, "The vibrational spectrum of tricarbonyl(trichlorostibine)nickel(0), [Ni(CO)$_3$(SbCl$_3$)]," *Journal of the Chemical Society, Dalton Transactions*, no. 3, pp. 681–682, 1987.

[21] T. Sasaki, S. Nishibe, H. Harima et al., "Raman study of low-temperature formation of nickel silicide layers," in *Proceedings of the 14th IEEE International Conference on Advanced Thermal Processing of Semiconductors (RTP '06)*, pp. 217–222, IEEE, Kyoto, Japan, October 2006.

[22] S. K. Donthu, D. Z. Chi, S. Tripathy, A. S. W. Wong, and S. J. Chua, "Micro-Raman spectroscopic investigation of NiSi films formed on BF$_2^+$-, B$^+$- and non-implanted (100)Si substrates," *Applied Physics A*, vol. 79, no. 3, pp. 637–642, 2004.

[23] M. Bhaskaran, S. Sriram, T. S. Perova et al., "In situ micro-Raman analysis and X-ray diffraction of nickel silicide thin films on silicon," *Micron*, vol. 40, no. 1, pp. 89–93, 2009.

[24] V. A. Solodukha, A. S. Turtsevich, Y. A. Solovyev, O. E. Sarychev, S. V. Gaponenko, and O. V. Milchanin, "Identification of nickel silicide phases on a silicon surface from Raman spectra," *Journal of Applied Spectroscopy*, vol. 79, no. 6, pp. 1002–1005, 2013.

[25] C. R. Das, H. C. Hsu, S. Dhara et al., "A complete Raman mapping of phase transitions in Si under indentation," *Journal of Raman Spectroscopy*, vol. 41, no. 3, pp. 334–339, 2010.

[26] P. J. Lin-Chung, "Local vibrational modes of impurities in diamond," *Physical Review B*, vol. 50, no. 23, article 16905, 1994.

[27] W. Windl, P. Pavone, K. Karch et al., "Second-order Raman spectra of diamond from ab initio phonon calculations," *Physical Review B*, vol. 48, no. 5, pp. 3164–3170, 1993.

[28] R. Brout and W. Visscher, "Suggested experiment on approximate localized modes in crystals," *Physical Review Letters*, vol. 9, no. 2, pp. 54–55, 1962.

[29] J. Isoya, H. Kanda, J. R. Norris, J. Tang, and M. K. Bowman, "Fourier-transform and continuous-wave EPR studies of nickel in synthetic diamond: Site and spin multiplicity," *Physical Review B*, vol. 41, no. 7, pp. 3905–3913, 1990.

[30] J. Isoya, H. Kanda, and Y. Uchida, "EPR studies of interstitial Ni centers in synthetic diamond crystals," *Physical Review B*, vol. 42, no. 16, pp. 9843–9852, 1990.

[31] V. A. Nadolinny, A. P. Yelisseyev, O. P. Yuryeva, and B. N. Feygelson, "EPR study of the transformations in nickel containing centres at heated synthetic diamonds," *Applied Magnetic Resonance*, vol. 12, no. 4, pp. 543–554, 1997.